IEEE Access
Multidisciplinary ⋮ Rapid Review ⋮ Open Access Journal

Received 18 July 2022, accepted 2 August 2022, date of publication 8 August 2022, date of current version 18 August 2022.

Digital Object Identifier 10.1109/ACCESS.2022.3197636

RESEARCH ARTICLE

Soil Water Content Estimation With the Presence of Vegetation Using Ultra Wideband Radar-Drone

ALOYSIUS A. PRAMUDITA[1], (Member, IEEE), YUYU WAHYU[2], SYAMSUL RIZAL[3], MURMAN D. PRASETIO[4], AGUNG N. JATI[3], RESTU WULANSARI[5], AND HARFAN H. RYANU[3], (Member, IEEE)

[1]Intelligent Sensing-IoT Center, Telkom University, Bandung 40257, Indonesia
[2]Telecommunication Research Center, BRIN, Jakarta Pusat 10340, Indonesia
[3]Electrical Engineering Faculty, Telkom University, Bandung 40257, Indonesia
[4]Industrial Engineering Department, Telkom University, Bandung 40257, Indonesia
[5]Tea and Cinchona Research Center, Bandung 40010, Indonesia

Corresponding author: Aloysius A. Pramudita (pramuditaadya@telkomuniversity.ac.id)

This work was supported by the Indonesia Endowment Fund for Education [Lembaga Pengelola Dana Pendidikan (LPDP)] of Indonesia through the Project of Rispro Invitasi 2021–2022.

ABSTRACT Radar–drone system is potentially implemented as a method for collecting the soil water content of a large area. Vegetation that may covers the soil surface affects the detection results of soil water content using radar system in plantation areas. Vegetation will influence the propagation mechanism of radar waves, therefore, a method to overcome this effect is needed. The method to compensate the effect of vegetation based on a transmission line model is then proposed in this paper. The transmission line model is used as the concept for transforming the measured reflection coefficient under the vegetation effect to the ground reflection coefficient value. Experiments were carried out by taking a case studies on tea plantations. The tea plant becomes a vegetation layer which its effect needs to be considered on the detection of soil water content. An ultra-wideband radar system with a frequency range of 500 MHz - 3 GHz is proposed in this study. The radar is integrated to hexacopter drone for scanning the tea plantation areas. The radar-drone system flight with a constant elevation from ground level. The experimental results show that the proposed method is able to improve the detection results of soil water content using radar with an accuracy of 96%. The radar-drone performance in detecting soil water content is suitable for precision farming purposes.

INDEX TERMS Soil water content, estimation, radar, drone, ultra wideband, vegetation effect.

I. INTRODUCTION

Soil is the top layer of the lithosphere that supports all life as the main component of terrestrial ecosystems. Soils are prone to degradation due to various reasons such as inappropriate land use, contamination from industrial waste, and other human activities [1]. The soil water content is an essential parameter that establishes the soil quality. The water content in the soil also reflects the ability of the soil structure to hold the water. Therefore, the potential flooding is possible to be mapped based on the ability of the soil to hold water. The water content of the soil is also an essential consideration in the field of civil construction. The water content in the soil will affect the growth of the vegetation and crop productivity [2]. Information on the water content in the soil is essential information to support precision farming systems [3], [4], [5]. Mapping the water content of the soil in an agricultural or plantation area is necessary for precision farming to deal with water and soil management.

Indonesia Statistic Center reported that tea is one of Indonesia's plantation commodities that continually grows [6]. Fertilization in tea plantations takes the most significant portion of production costs (40-60%). The data of soil water content becomes a reference for determining the timing of fertilization and the amount of fertilizer. Therefore, the effectiveness and efficiency of fertilization can be optimized. Currently, the soil water content data in Indonesian tea plantations is only estimated from rain-fall data. These data are not accurate enough to represent the soil water content data that is needed in the fertilization process. Methods for

The associate editor coordinating the review of this manuscript and approving it for publication was Pinjia Zhang.

estimating soil moisture content for large areas such as tea plantations are then needed to support precision fertilization.

Several methods for measuring soil water content can be categorized into two types: direct and indirect. Gravimetric is categorized as a direct method [5], [7]. The soil sample in a certain location is taken, and measure the difference between fresh and dried weights. In most studies, the Gravimetric result is used as ground truth in developing a new measurement method of soil water content. Indirect methods are developed based on physical behaviour such as resistive, capacitive, time domain reflectometry, and electromagnetic wave. The gravimetric method will consume much time for many samples required in extensive area observation. Some soil water content sensors, such as resistive and capacitive sensors, are used by invasive operations, and many sensors are therefore needed for extensive area observation. The remote sensing method for estimating soil characteristics then becomes a method that continues to be studied for mapping soil conditions over a large area. The wave propagation phenomenon is generally used as a basic concept in the remote sensing method. These remote sensing methods include satellite imaging [8], [9], [10], Synthetic Aperture Radar (SAR) [11], [12], [13], [14], radiometry [15], Time domain reflectometry (TDR) [16], [17], [18], [19] and Ground Penetrating Radar (GPR) [20], [21], [22], [23], [24], [25]. The measurement result from a contact or invasive sensor such as a TDR is limited to a certain point in representing the soil water content. A large number of sensors will be needed to monitor a large area. The previously proposed use of satellite imagery, radiometry, and SAR is capable of covering a large area of observation. How-ever, the accuracy that can be achieved is inadequate as the data used for precision farming. Limited power on a large distance measurement causes the electromagnetic wave to be difficult to penetrate the vegetation covering the plantation area. Ground Penetrating Radar (GPR) is a system for detecting objects buried under the ground surface by utilizing the phenomenon of electromagnetic waves. GPR technology demonstrates its capability to collect data for a large area by conveying the GPR device to scan the observed area. Many studies in GPR have shown the effect of soil conditions on the detection results [26], [27]. These facts motivate the development of GPR applications to measure the soil water content and topsoil thickness over a large area [28]. Several studies were also intended to improve the detection result by making an effort both in the processing part [23], [29], [30] and hardware [31]. The limitations of the GPR system are generally due to the simplification of the assumptions related to radiation and wave propagation that occurs. Only some part of the information is utilized in the waves [32]. Furthermore, the relevant wave propagation modelling on the GPR system to extract more detailed information is required. Previous research on the model of extracting information on the soil water content and thickness of the topsoil layer has been conducted. The extraction model has been formulated based on the potential propagation model. The theoretical and numerical simulation studies have been performed [28], [33].

Recently, the integration of the GPR system on the drone is exciting research, and many studies in this field have been performed, i.e., landmine detection [34], [35], [36], snow cover mapping [37], human detection [38], and earth surface survey [39]. In this paper, the integration of UWB radar and hexacopter drone is proposed as a method for measuring the soil water content of plantation areas. The hexacopter conveys the UWB radar in collecting the soil water content data over a large area. In a number of soil water content detection cases using radar, it is often found that the soil surface is covered by vegetation. This case is often found in agricultural or plantation areas. Vegetation that covers the ground surface will influence the propagation of radar waves. Therefore, the detection results are potentially influenced by the presence of the vegetation. Methods to accommodate the effect of vegetation are needed to improve the accuracy of the detection results. Based on the author's best knowledge, only a few studies have been conducted to overcome the vegetation effect problem in measuring soil water content using GPR. From Through the Wall radar field, we can learn that the effect of the wall as a barrier to the target detection process became a critical issue to investigate, and the methods were developed to overcome this effect [40], [41]. The problem addressed in this research is to improve the accuracy of the proposed UWB radar-drone in detecting soil water content with the presence of vegetation over the ground surface. The inference method based on the transmission line model is proposed to improve the detection accuracy while respecting the effects of the vegetation layer. The proposed inference method becomes part of radar-drone processing. A study on a tea plantation was con-ducted to evaluate the capability of the proposed method. The discussion in the paper is structured as follows: In the introduction section, the problems raised as motivations for developing the proposed method are described. Then in the second part, the wave propagation model and the compensation method are described based on the transmission line model. In the third section, the experimental methods and discussion of the results obtained are explained, and finally, the conclusions.

II. MATERIALS AND METHODS

A. RADAR-DRONE FOR SOIL WATER CONTENT ESTIMATION ON TEA PLANTATIONS

The implementation of a radar system for the estimation of water content in soil is based on the concept of electromagnetic wave propagation crossing the boundary between different mediums, where the electrical characteristics of the soil determine the radar signal reflected by the soil surface. The TOPP model describes the relationship between the water content of the soil and the permittivity of the soil [42]. Fig. 1 shows the relationship curve between soil permittivity and water content in the soil. Based on this relation, when the radar receives the reflected signal from the ground surface, the permittivity of the ground can be estimated from the intrinsic impedance of the soil, which formerly can be

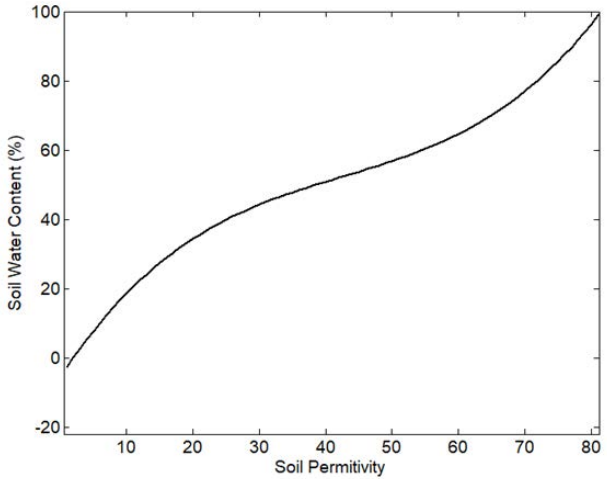

FIGURE 1. Relationship between soil permittivity and water content in the soil referring the TOPP formula in [42].

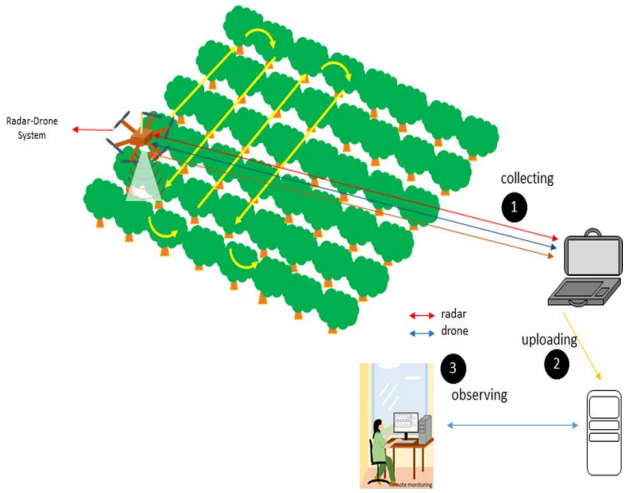

FIGURE 2. Illustration of proposed UWB radar-drone implementation.

calculated referring to the reflection coefficient obtained from radar signal. The water content in the soil is then estimated using the TOPP model equation.

In order to collect the soil water content data over a large area, the radar is integrated with a hexacopter drone system. The pathway of the hexacopter in conveying the radar can be controlled for scanning purposes. The drone Fig. 2 illustrates the concept of radar-drone implementation for soil water content estimation over tea plantation proposed in this paper.

The radar system proposed in this study is a UWB radar developed based on a stepped frequency continuous wave topology. Several studies on the radar application report that the electromagnetic wave in the L-Band frequency range is potentially used to penetrate the vegetation layer [15], [43], [44], [45]. Considering the results of these studies, UWB Radar is designed in the L-Band frequency range. In this research, the SFCW radar system was realized to operate with a frequency range between 500 MHz to 3 GHz. Respecting the capability of the Vector Network Analyzer (VNA) for radar modelling reported in [46], the Mini VNA was employed as the transceiver part of the radar. The first port

TABLE 1. Proposed radar dimension and its performance.

Dimension	Value (mm)	Parameter	Performance
L1|L2|L3	295|400|52.5	Freq.Range	500 MHz - 3 GHz
S1|S2	78|70	Transmit Power	-14 dBm
W1|W2|W3	220|220|140	Weight	2.3 Kg
M1|M2|M3|M4	20|130|150|195	Radiation	Directional
a|b	56|44.8	Ringing Level	<-30 dB after 35 cm
f1|w	130|30|60		
Substrate	R04003		
Thickness	0.8		

is operated as the transmitter, and the second port is operated as the receiver. The transmitter and receiver ports are then connected to the UWB antenna, which is designed with a self-complementary ellipsoid structure. The antenna has a directional time-domain radiation pattern and also contributes low ringing level. The Mini-VNA has a transmitted power of 14 dBm. The transmit power is still sufficient for a view meter detection range. When a more extended detection range is required, the power amplifier can be installed on the transmitter side, and the Low Noise Amplifier can be installed on the receiver. In the proposed radar design, the mini-pc is used as a processing unit that serves the data acquisition, received signal reconstruction, inference method computation, and result representation. The rechargeable battery with an output voltage of 12 V and capacity of 2000mAh is used as a radar power supply. The total weight of the radar that is included the casing and material handling structure is about 2.3 kg. The proposed UWB radar system design with SFCW topology and the prototype realization is shown in Fig. 3. The proposed radar dimensions and specifications are summarized in Table 1.

The SFCW signal generated in the proposed radar system can be written as (1). With f_0, N, and Δ_f respectively as the lowest frequency, the number of steps and the step size between the frequency components in SFCW. A_n and θ_n are the amplitude and phase of the frequency component. For synthesizing a particular signal, the values of A_n and θ_n can be determined based on the magnitude and phase of the signal Fourier transform. Monocycle pulse is the first derivative of Gaussian pulse that exhibits a low dc level. This study chose the monocycle signal as the radar signal, which was synthesized using the SFCW technique. The monocycle signal equation is written as (2), with σ and τ representing the monocycle parameter that is used to determine the pulse width.

$$X_T(t) = \sum_{n=1}^{N+1} A_n cos(2\pi(f_0 + (n-1)\Delta_f) t - \theta_n) \; for \; (n-1)T \ll t < nT \quad (1)$$

$$X_{mono}(t) = \frac{1}{\sigma^3\sqrt{2\pi}}(t-\tau)e^{\frac{(t-\tau)^2}{2\sigma^2}} \quad (2)$$

The first and second port of the Mini-VNA respectively functions as a transmitter and a receiver of the proposed radar system. Suppose the X_R is the detected signal on the mini-VNA receiving port. In that case, the scattering parameter data S_{21} measured is the transfer function from X_T

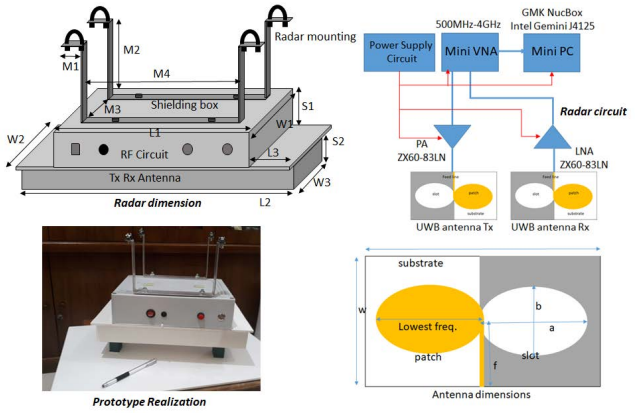

FIGURE 3. UWB stepped frequency design.

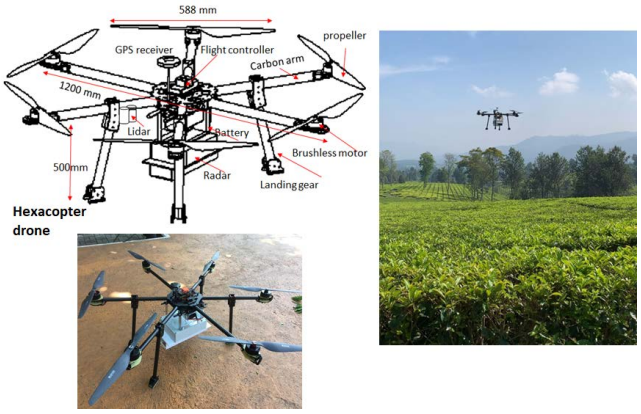

FIGURE 4. Hexacopter drone design that integrated with UWB radar system.

to X_R. Mini-VNA is controlled by the software designed to regulate the generation and reception of SFCW signals. The S_{21} data obtained from the Mini-VNA is a sequence on the frequency domain as written as (3). However, the obtained data must be compiled into the correct FFT sequence. The arrangement can be written in (4). Zero padding is performed when the S_{21} sequence (N) length is smaller than the desired FFT sequence. Furthermore, the received signal can be reconstructed by calculating the inverse Fast Fourier Transform that is written in (5). The steps of reconstructing the received signal from the measured S_{21} data have been explained in [46].

$$S_{21} = [S_{21}(1)S_{21}(2)S_{21}(3)\ldots S_{21}(N)] \tag{3}$$

$$S_{21k} = [0S_{21}00\ldots S_{21}^{*}0] \tag{4}$$

$$X_R = F^{-1}[S_{21}(f)X_T(f)] \tag{5}$$

The drone system is designed with a hexacopter structure for a maximum payload of 5 kg. The hexacopter drone will convey the radar system in collecting the soil water content data over the observation area. Hexacopter is controlled to fly at a relatively constant altitude above the ground surface. The constant altitude flight is expected to maintain the radar signal power uniformity that reaches the ground surface. The drone is constructed from several principal components such as the 380 kV Brushless motor, 558 mm propeller, Pixhawk 2.1 Cube flight controller, GPS receiver, and 16000 mAh battery. A telemetry system is used for monitoring the drone flight data. It operates at a frequency of 433 MHz and has up to a 2 km range. The wireless remote control is also served for manual operation. The height of the tea plant ranges from 50 cm to 100 cm, and the drone is controlled to convey the radar system at a constant altitude of 2 m. The design and photo of the drone prototype that has been integrated with the radar are shown in Fig. 4.

B. PROPOSED INFERENCE METHOD

The inference method is part of the radar data processing that the mini-pc handles the computation. The inference method is used to process the reconstruction of the received signal in obtaining the soil water content information. The proposed inference method is derived from the propagation model of the radar wave through several different mediums. Fig. 5(a) illustrates the wave propagation of a radar system when detecting water content in the soil without the presence of vegetation. The intrinsic impedance of the ground determines the reflection from the ground surface. When the medium between the radar and the ground is air, the reflection coefficient will be negative [47]. By assuming that the intrinsic impedance of the air is represented by free space, then the soil permittivity data can be obtained based on the value of the reflected coefficient. The soil water content is then estimated using the TOPP model equation as discussed in [42]. Fig. 5(b) illustrates the situation of soil water content measurement using radar which is carried out in a condition where the soil is covered by vegetation. It can be found in tea plantations, where most of the soil is covered by tea plants. In this situation, the measured reflected coefficient certainly does not fully represent the reflection coefficient at the ground surface. The waves from the radar will propagate through the vegetation layer. Only some of the waves reach the boundary of the soil surface. Likewise, reflected waves from the ground surface will propagate through the vegetation layer before reaching the radar system receiver. The vegetation layer's electrical characteristics and the vegetation's height will influence the reflected coefficient measured by the radar system. This research aims to develop a method for overcoming the effects of the vegetation layer's electrical characteristics and the vegetation's height on detection accuracy.

Radar wave propagation in situations where a layer of vegetation covers the ground can be categorized as wave propagation in the layered medium, as illustrated in Fig. 5(b). It is illustrated that there are three layers of medium related to the propagation of radar waves. The first medium is air, the second medium is a layer of vegetation, and the third medium is soil. In several cases, the radar wave propagation through several mediums, then efforts to improve performance or overcome the problem of the barrier medium are necessary to carry out. For example, the wall is a barrier medium between the radar and the target in the through-the-wall radar cases.

Methods to overcome the effect of the barrier wall are then proposed to improve the results [40], [41].

A transmission line model has been proposed in a previous study to analyze electromagnetic wave propagation in a layered medium [47], [48]. In this research, the transmission line model for the layered medium is studied as a radar electromagnetic wave propagation model in the case of Fig. 5(b). Based on this model, a method is obtained to transform the reflection coefficient of the radar measurement results into the reflection coefficient from the ground surface. The transmission line model to describe the propagation of radar waves in the detection of soil water content in the presence of vegetation barriers is shown in Fig. 5(b). Γ_{meas} is the reflection coefficient obtained from the radar detection result calculation. The value will represent the reflection coefficient of the soil when there is no covered vegetation. The value cannot accurately represent the soil reflection coefficient when there is covered vegetation. As written in (6), the measured reflection coefficient is determined by the air's intrinsic impedance and the vegetation layer's impedance in the boundary plane as written in (1). $Z_v(-d)$ is the impedance of the vegetation layer on the boundary plane between vegetation and the air. The value is determined not only by the vegetation's characteristics but also by the height of the vegetation. η_{air} is the intrinsic impedance of the air.

$$\Gamma_{meas} = \frac{Z_v(-d) - \eta_{air}}{Z_v(-d) + \eta_{air}} \tag{6}$$

Manipulation of equation (1) can then be performed to obtain the value of $Z_v(-d)$. The $Z_v(-d)$ value can then be determined based on (7).

$$Z_v(-d) = \frac{(1 + \Gamma_{meas})\eta_{air}}{(1 + \Gamma_{meas})} \tag{7}$$

Based on the transmission line model in Fig. 5(b), the value of $Z_v(-d)$ is determined by the intrinsic impedance of the vegetation layer (η_v) and the reflection coefficient at the boundary of the vegetation layer $\Gamma_v(-d)$. The relation is written in (8). After $Z_v(-d)$ is obtained from $Z_v(-d)$, the $\Gamma_v(-d)$ can be calculated using (9). The $\Gamma_v(-d)$ is the reflection coefficient of the ground surface observed at a distance d from the ground surface. The value is influenced by the electrical properties of the vegetation layer. The influence can be expressed in terms of propagation constant. In calculating the reflection coefficient on the ground surface (Γ_{soil}), it is necessary to determine the vegetation reflection coefficient first x. Then the reflection coefficient $\Gamma_v(-d)$ can be determined by referring to (9). Furthermore, the calculation of Γ_{soil} can be written as (10).

$$Z_v(-d) = \eta_v \frac{(1 + \Gamma_v(-z))}{(1 - \Gamma_v(-z))} \tag{8}$$

$$\Gamma_v(-d) = \frac{Z_v(-d) - \eta_v}{Z_v(-d) + \eta_v} \tag{9}$$

The height of the vegetation (d) is essential information that must be obtained before carrying out calculations (10).

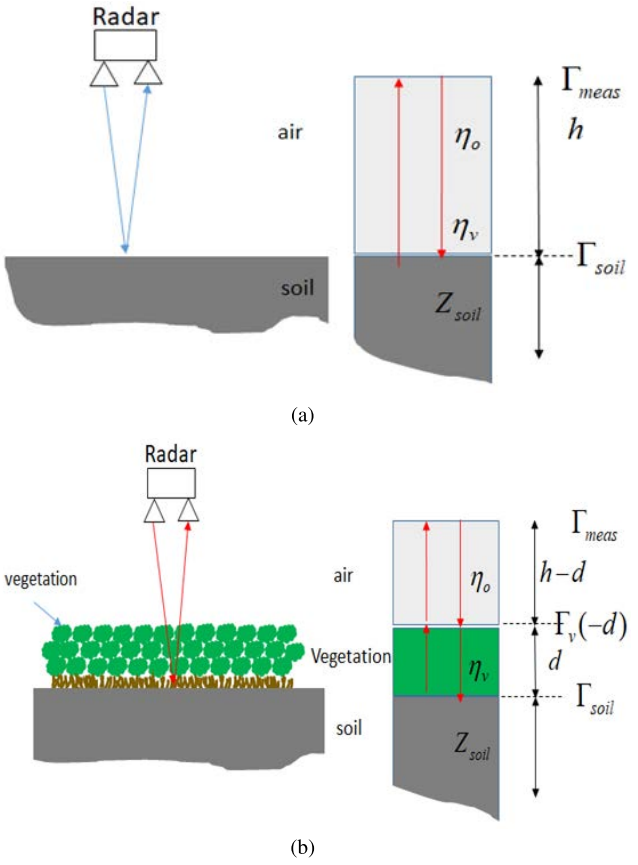

FIGURE 5. Illustration of the use of radar for estimation of water content in soil. (a). without any vegetation barrier. (b) with barrier vegetation.

Vegetation height can be obtained by detecting the delay in the reflected signal passing through the vegetation layer. Based on the delay, the height of the vegetation can be estimated. Then the actual ground reflection coefficient can be calculated using (10). α and β are the propagation constant in the vegetation layer, which has been estimated based on a series of measurements made in the plantation area. Values are obtained by calculating the average attenuation and phase shift of several measurements representing vegetation in the plantation area.

$$\Gamma_{soil} = \Gamma_v e^{2(\alpha + j\beta)d} \tag{10}$$

The α and β measurements were performed using the scenario shown in Fig.6 to estimate the α and β values of the vegetation layer. Measurements are taken by placing the radar at a constant elevation of 2 m above ground level, which is facilitated by a support structure as shown in Fig.6a. The reflected signal is taken for two conditions, i.e., without a vegetation layer and with the vegetation layer. During measurement, the ground surface is covered with an aluminum foil to provide maximum reflection in these measurements. Fig 6 also shows a photograph of the measurement situation on a tea plantation. The reflected signal difference obtained from with and without vegetation layer is related to the presence of a layer of vegetation. Fig.7 shows an example of the radar

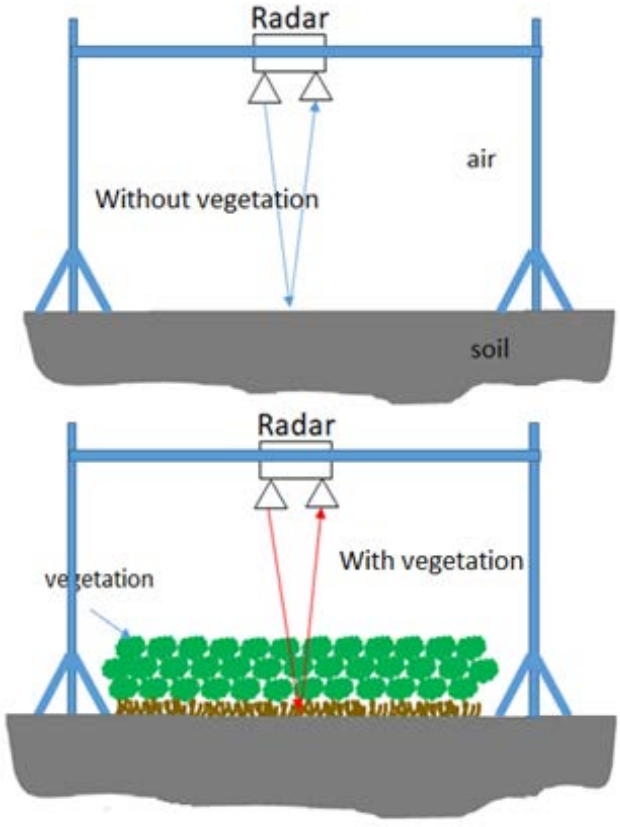

(a)

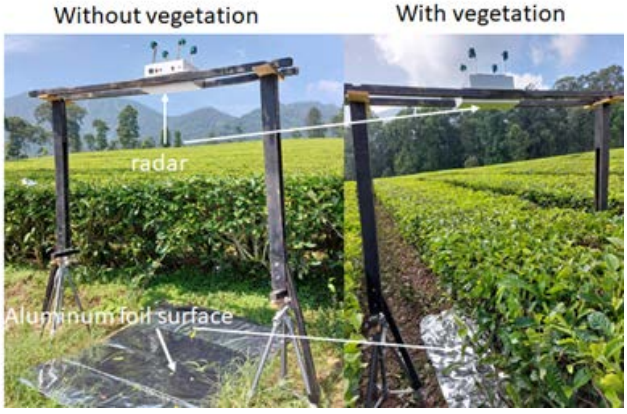

(b)

FIGURE 6. Measurement setup of α and β. (a) Measurement setup. (b) Photograph of measurement setup at tea plantation.

reflected signal resulting from the measurement illustrated in Fig 6. The total attenuation of the vegetation layer with a certain height can be obtained from the peak amplitude comparison of the reflected signal from conditions with and without vegetation. As shown in Fig.7, when X_{rwo} and X_{rw} represent the peak amplitude of reflected signal from without and with vegetation scenario, then the $|X_{rw}/X_{rwo}|$ represents the vegetation layer attenuation. Furthermore, the Furthermore, α_v can be determined from the attenuation value. Based

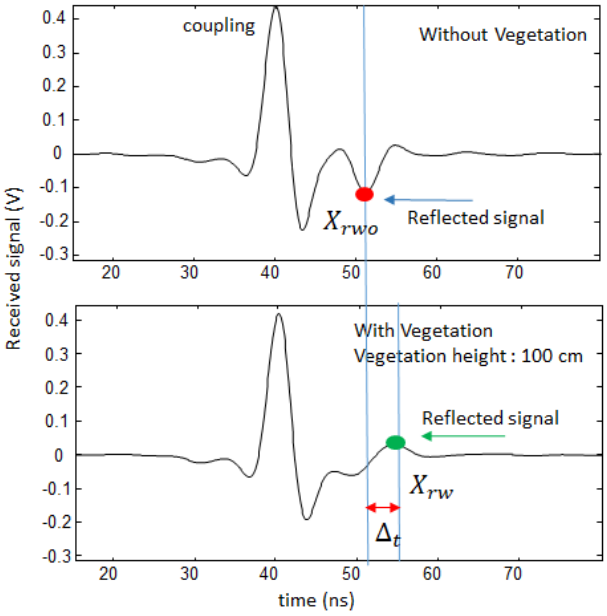

FIGURE 7. Illustration of reflected signal obtained from with and without vegetation layer condition.

on the time difference of the reflected signal (δ_t) the total phase shift can be obtained. The β can be determined from the obtained phase shift. α_v and β_v values in vegetation layer can be determined by equations (11) and (12) with ω, μ, ϵ and σ are respectively as angular frequency of radar signal, permeability, permittivity and conductivity of vegetation layer. Therefore, the electric properties of the vegetation layer can be determined from the obtained α_v and β_v.

$$\alpha_v = \omega\sqrt{\mu\epsilon}\left(\frac{1}{2}\left[\sqrt{1+\left(\frac{\sigma}{\omega\epsilon}\right)^2}-1\right]\right)^{\frac{1}{2}} \tag{11}$$

$$\beta_v = \omega\sqrt{\mu\epsilon}\left(\frac{1}{2}\left[\sqrt{1+\left(\frac{\sigma}{\omega\epsilon}\right)^2}+1\right]\right)^{\frac{1}{2}} \tag{12}$$

When we replace the $\sigma/\omega\epsilon$ value with x, then the x value can be calculated based on the ratio of α_v and β_v. Let us define the ratio of α_v and β_v as written in (13). Then x can be written as (4).

$$\frac{\alpha_v}{\beta_v} = \frac{\left[\sqrt{1+x^2}-1\right]^{\frac{1}{2}}}{\left[\sqrt{1+x^2}+1\right]^{\frac{1}{2}}} \tag{13}$$

$$x = \left[\frac{1+\left(\frac{\alpha_v}{\beta_v}\right)^2}{1-\left(\frac{\alpha_v}{\beta_v}\right)^2}-1\right]^{\frac{1}{2}} \tag{14}$$

After x is obtained through (14) and substituting x into (12), the ϵ can be determined by assuming that the vegetation layer is non-magnetic. By recalling that x is $\sigma/\omega\epsilon$, the conductivity value can be calculated after ϵ is obtained. After the electric properties of the vegetation are obtained, the characteristic impedance of the vegetation layer η_v required in the calculation (8) dan (9) can be calculated based on (15).

$$\eta_v = \sqrt{\frac{\mu}{\epsilon(1-jx)}} \tag{15}$$

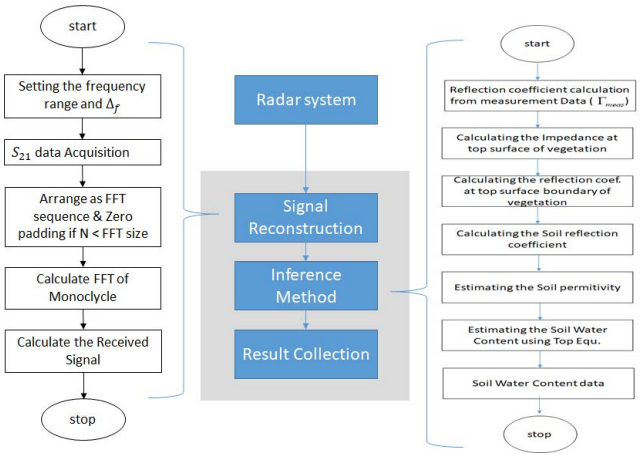

FIGURE 8. Processing part of proposed radar system.

The next step is to calculate the permittivity of the soil based on the value of the soil reflection coefficient obtained from (10). The calculation is carried out based on (16). Furthermore, the estimated soil water content can be calculated using the TOPP Model equation written in (17).

$$\hat{\varepsilon}_{soil} = \varepsilon_v \frac{(1-\Gamma_{soil})^2}{(1+\Gamma_{soil})^2} \tag{16}$$

The radar signal processing that elaborates the proposed inference method is described in Fig. 8. The inference method considers the vegetation effect and is computed after the received signal reconstruction process. The soil water content estimation resulting from inference method computation is then collected and can be used for precision farming purposes.

$$\hat{m}_v = 5.3x10^{-2} + 2.92x10^{-2}\hat{\varepsilon}_{soil} - \hat{\varepsilon}^2_{soil}5.5x10^{-4} + \hat{\varepsilon}^3_{soil}4.3x10^{-6} \tag{17}$$

In assessing the proposed method's ability, a series of experiments were carried out at a tea plantation located in Ciwidey West Java, Indonesia. Three different tea plantation blocks are used in the experiment. The data of each plantation block are listed in Table 2. The experiment is performed for two types of measurement mechanisms. The first type is a measurement conducted by hovering the drone at a selected location in a plantation block. The drone is controlled to keep the constant elevation of 2 m when the measured data are collected. The second type is a measurement conducted with a particular pathway determined for scanning the observation area. In the second type of measurement mechanism, the GPS data is also recorded for every measurement point. The Gravimetric is employed as a ground truth invalidating the measurement. The measurement in every block is also taken two different times.

III. RESULTS AND DISCUSSION

The simulation was conducted for a preliminary investigation of covered vegetation's influence on the radar detection

TABLE 2. The data of plantation block that taken as experiment object.

Data	Block I	Block II	Block III
Vegetation	Tea	Tea	Tea
Average Height	70 cm	90 cm	60 cm
Location	-7.14748, 107.50906	-7.15535, 107.50665	-7.14385, 107.51117

result. In this simulation, soil water content is estimated by assuming the reflection coefficient obtained from radar reflected signal is the reflection coefficient of the soil surface. The simulation is conducted for several different vegetation heights and vegetation attenuations. The results are depicted in Fig. 9. The red line is the estimated soil water content when no vegetation cover indicates the correct result. Fig. 9(a) and Fig. 9(b) show that the presence of vegetation layer in the detection process causes the deviation in the estimated soil water content from the correct result. The deviation increases as the attenuation increases. The results also show that the higher vegetation height provides a higher deviation from the correct result.

After studying the vegetation effect by conducting a computer simulation, several drone-radar prototype experiments are performed on the tea plantation. The first experiment was carried out at several locations on the tea plantation, which have different vegetation heights. Fig. 10 shows the results of received signal reconstruction from measurements made under different conditions. The radar-drone elevation is 2 m from the ground surface. The top graph shows the received signal in the absence of cover vegetation. The received signal consists of a coupling signal (direct propagation from transmitter to receiver antenna) and a reflected signal from the soil surface. The position of the coupling signal can be used to determine the position of the radar.

Furthermore, it is used as a reference point to estimate the target's distance. The distance of the reference point to the peak of the reflected signal represents the target's distance from the radar. For example, the peak of the reflected signal in the top graph has a distance of 13 ns from the coupling signal. Therefore, the estimated propagation distance is about 3.9 m, and the radar distance from the ground is half of this value. The second and third graphs show the received signal when the measurements are taken at two different vegetation heights, i.e., 60 cm and 90 cm. Both of these results indicate that the position of the reflected signal shifted away compared to the result in the first graph. The reflected signal has a tremendous shift when the measurement is taken in the higher vegetation condition. These results indicate that the presence of vegetation causes a phase shift so that the soil surface distance to the radar seems to be farther away. The results also show that the presence of vegetation reduces the peak level of the reflected signal. The results in Fig. 10 indicate that vegetation on plantations affects changes in the amplitude and phase shift of the reflected signal. Fig. 9 and Fig. 10 confirm that the vegetation layer's influence on the radar's reflected

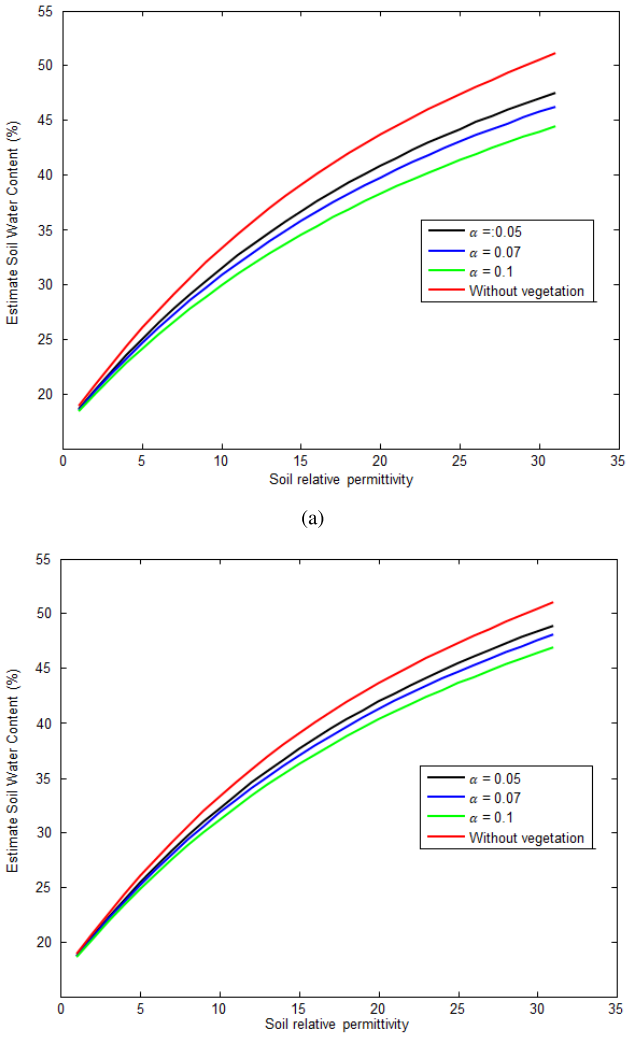

FIGURE 9. Effect of vegetation attenuation and height to the soil water content estimation result. (a). Vegetation height = 90 cm. (b) Vegetation height = 50 cm.

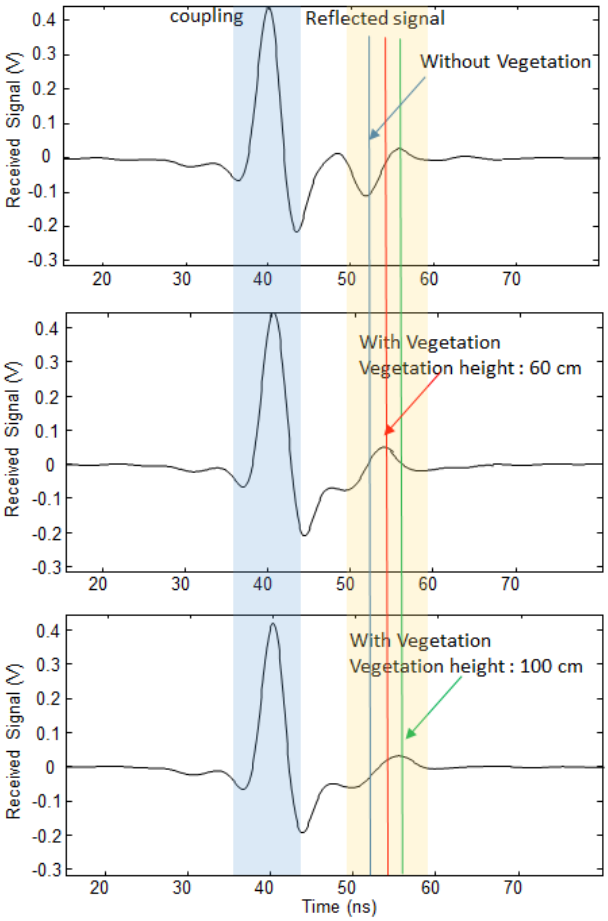

FIGURE 10. Received signal at three different condition of vegetation layer with the radar elevation of 2 m.

signal needs to be considered in the detection process. If the obtained results are directly used to determine the reflection coefficient from the ground, the results can be inaccurate. Gravimetric is carried out on a number of soil samples in the Block to be observed. The sample location is the same as the hovering location of the radar drone. When performing experiment, six soil samples were taken for each Block in Tabel.2, and each sample was taken as much as 300 grams. Gravimetric results are used to validate the measurement results using drone radar.

After the received signal is obtained from the reconstruction process, the next step is to remove the coupling signal. The coupling signal removal is performed by subtracting the received signal from the received signal that has been recorded when the radar is aimed at free space (no reflected signal component). After subtraction, the received signal residue will only leave part of the reflected signal. Therefore, the reflected signal is easier to detect. By performing peak detection, the reflected signal components can be identified. As previously explained in section 2, the UWB signal synthesized using SFCW is in the form of a monocycle. Furthermore, the reflected signal's peak to peak amplitude value is then used to determine the reflection coefficient. Fig. 11 shows some samples of the received signal reconstruction results. For example, Fig. 11(a) is the result of the received signal reconstruction when the experiment is conducted on Block-I, with the height of the tea plant is 75 cm and the soil water content of the gravimetric is 35%. The obtained reflected signal is then represented in absolute value as shown in Fig. 11(b) on the graph with the red line. By converting the signal representation into absolute form and followed by peak detection, the positive and negative peaks of the reflected signal can be identified as two consecutive peaks. The location of the reflected signal is defined as the midpoint between the first and second peaks. Then the measured reflection coefficient value can be determined to compare the peak-to-peak value of the reflected signal with the peak to peak value when total reflection occurs. Fig. 11(c) is reconstructing the received signal in the experiment conducted in Block-II

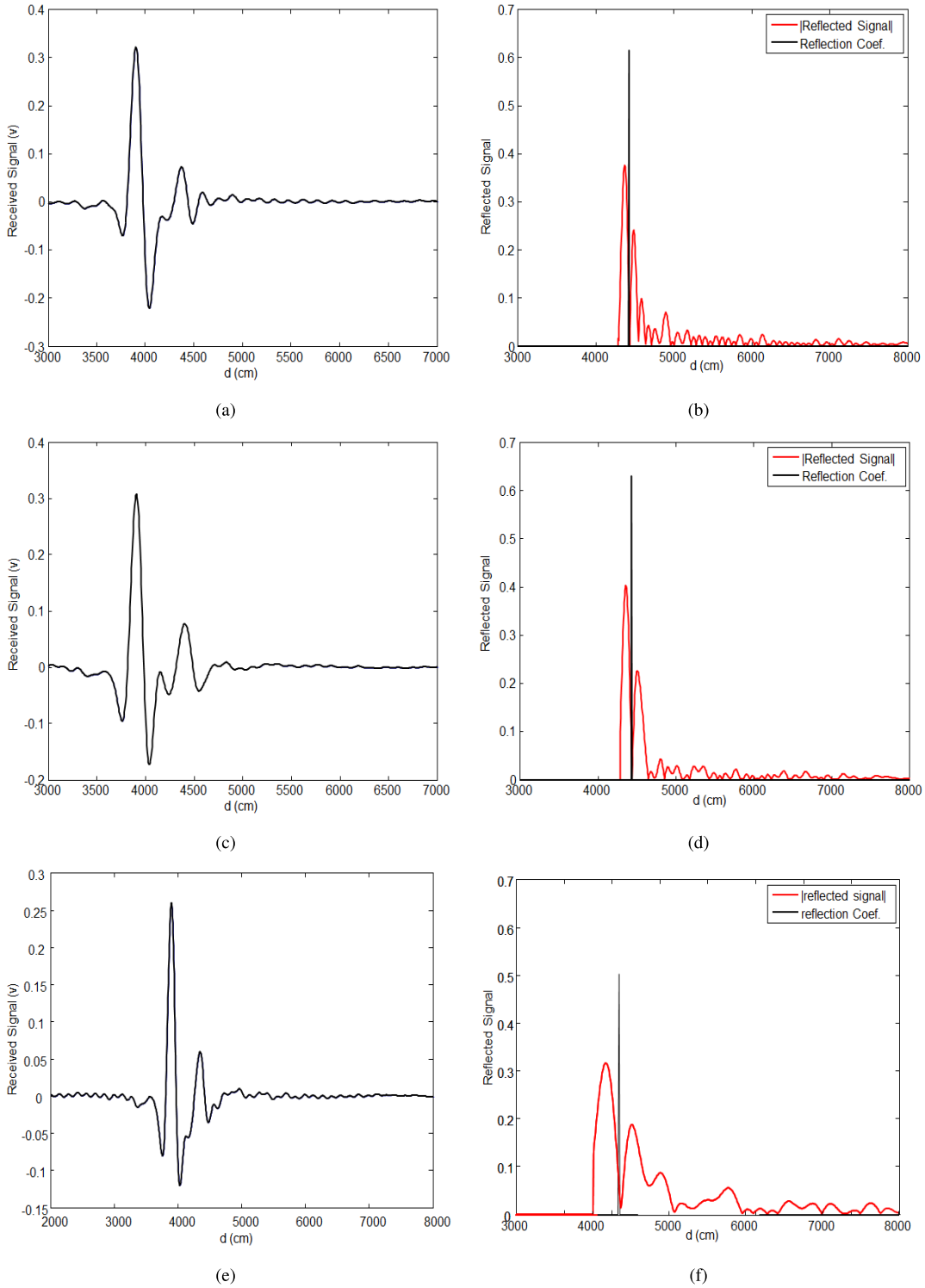

FIGURE 11. Sample of Reconstructed received signal and the reflected signal. (a). Received signal from Block I. (b). Reflected signal from Block I. (c). Received signal from Block II. (d). Reflected signal from Block II. (e). Received signal from Block III. (f). Reflected signal from Block III.

with a tea plant height of 90 cm and a soil water content of 45% from Gravimetric. Figure 11(d) is the reflected signal in the absolute form obtained after subtracting the signal to ward free space. Fig. 11(e) and Fig. 11(f) is the result for the Block-III with a tea plant height of 60 cm and a soil water content of 30%.

After the measured reflection coefficient is obtained, the next step is to estimate the value of the soil water content.

Estimation of soil water content based on the measured reflection coefficient is carried out by calculating the inference method that has been proposed in section 2. The calculation process is carried out sequentially, referring to the flowchart in Fig. 6. The calculation process for each step follows equations (7) to (17). The characteristics of wave propagation in vegetation represented by α and β, as written in (10) need to be obtained first. The static measurement as illustrated in Fig.6 are performed to estimate α and β. Several measurements using the designed radar were carried out for several plant heights. The average value of the overall results that have been collected is then used to determine the α and β values of the tea plant. The result shows that the α and β of the tea plant are 1.2 Np/m and 31 rad/m.

After the estimated soil permittivity is obtained, the estimated value of the soil water content can be determined based on the Top model equation in (12). Fig. 12 shows the estimation results of soil water content by applying the proposed inference method. These results were obtained in experiments carried out on three different blocks, namely Block I, II, and III whose conditions have been described in Table 2. The results are obtained by flying the radar-drone to the selected location as a sample, and data collection is carried out when the drone is hovering. Each result in Fig. 10 compares the estimation results obtained by applying the proposed method with the estimation results that ignore the presence of vegetation. Gravimetric is also performed, and the results are used as ground truth to evaluate the accuracy of the estimation results. Several measurements were taken at each Block and conducted at several different times. The proposed method shows better accuracy than the results that ignore the presence of vegetation. The maximum deviation of the estimation results by applying the proposed method is 4%. The estimation accuracy reaches 96%. The total root mean square error (RMSE) obtained from all measurement is about 2.28%. The results obtained from several experiments conducted at the exact location and time indicate fluctuations. That is due to height fluctuations of the drone when hovering. Altitude data recorded through the telemetry facility of the drone shows that the average height deviation from the drone is 6 cm. However, the estimation results of soil water content achieved by the proposed method are still tolerable for precision farming.

The landscape of tea plantations has variations in height. The variations are also caused by plantation management needs or due to crop damage. The path for the picking and pruning process is not covered by plants. At several locations, plant damage was found which the vegetation height to be different from the surrounding. The existence of landscape variations causes the results of the lidar sensor on the radar to be sensitive to these conditions and cause fluctuations in the drone's flying height. Fig. 13 shows a sample of soil water content detection results collected at several points when the drone flies over the tea plant. Several outlier data are found in the measurement result. The outlier data are caused by unusual vegetation cover conditions, such as due to special pruning or crop damage. Outlier data will then be removed from the detection results.

Testing the proposed drone radar system to estimate soil water content in a large area has also been carried out. For each experimental sample area, the flying trajectory of the drone is determined first. Then the estimation results are presented in the form of a bubble map. The estimation results are plotted according to the recorded position of the installed GPS receiver. Fig. 14 shows the estimation results at several points obtained when the radar drone is flown to scan two different sample areas. For example, in Fig. 14(a) radar-drone is used to scan an area of 20 m $\times$ 40 m. The flight time required is about 5 minutes 20 seconds. With a 16000 mAh battery that can support a flight time of about 15 minutes, the total area that can be scanned is 2250 m^2.

Soil water content information has an important role in several aspects of plantation management. SWC estimation method that is fast and accurate in collecting the estimation result is necessary to apply precision farming. Radar-drone is a promising method for achieving this capability. Its ability to collect soil water content data over a large area with high accuracy is very relevant to the needs of precision farming. The Gravimetric [5], Conductive [50], Capacitive [51], and TDR [16], [17], [18], [19] methods are commonly operated as the invasive method. In the plantation case, when a vegetation layer covers the soil surface, the invasive method is less support in collecting measurement data for a large area. Many samples or sensors are required to obtain data over a large area where the distribution of soil water content varies. Techniques for collecting detection results from each sensor also need to be provided. It is the drawback of these methods. However, the high measurement accuracy of Gravimetric methods then becomes a consideration as ground truth. Remote sensing methods such as satellite imagery [8], [9], [10] and SAR [11], [12], [13], [14] can support collecting the soil water content data from a large area. However, to increase detection accuracy in the presence of vegetation effects, it is necessary to develop a fairly complex processing technique. In addition, technology investment for implementing these methods is also expensive. UWB radar-drone, as the proposed method, can collect soil water content data quickly for a large area. The inference method has accommodated the effects of vegetation. Although the method was developed for the case of tea plantations, the method can be customized for plantations with other vegetation types.

Fig. 10 and Fig. 11 show that the UWB radar with a frequency around L-Band can identify reflections from the ground surface even though there is a vegetation layer over the soil surface. However, plants covering the soil surface significantly influence obtaining the accurate soil water content estimation result. The vegetation layer will provide attenuation and phase shift of the radar signal. The amount of attenuation and phase shift is determined by the type of vegetation and the height of the plant. The attenuation of the tea plant causes the reflected signal to be smaller than the coupling

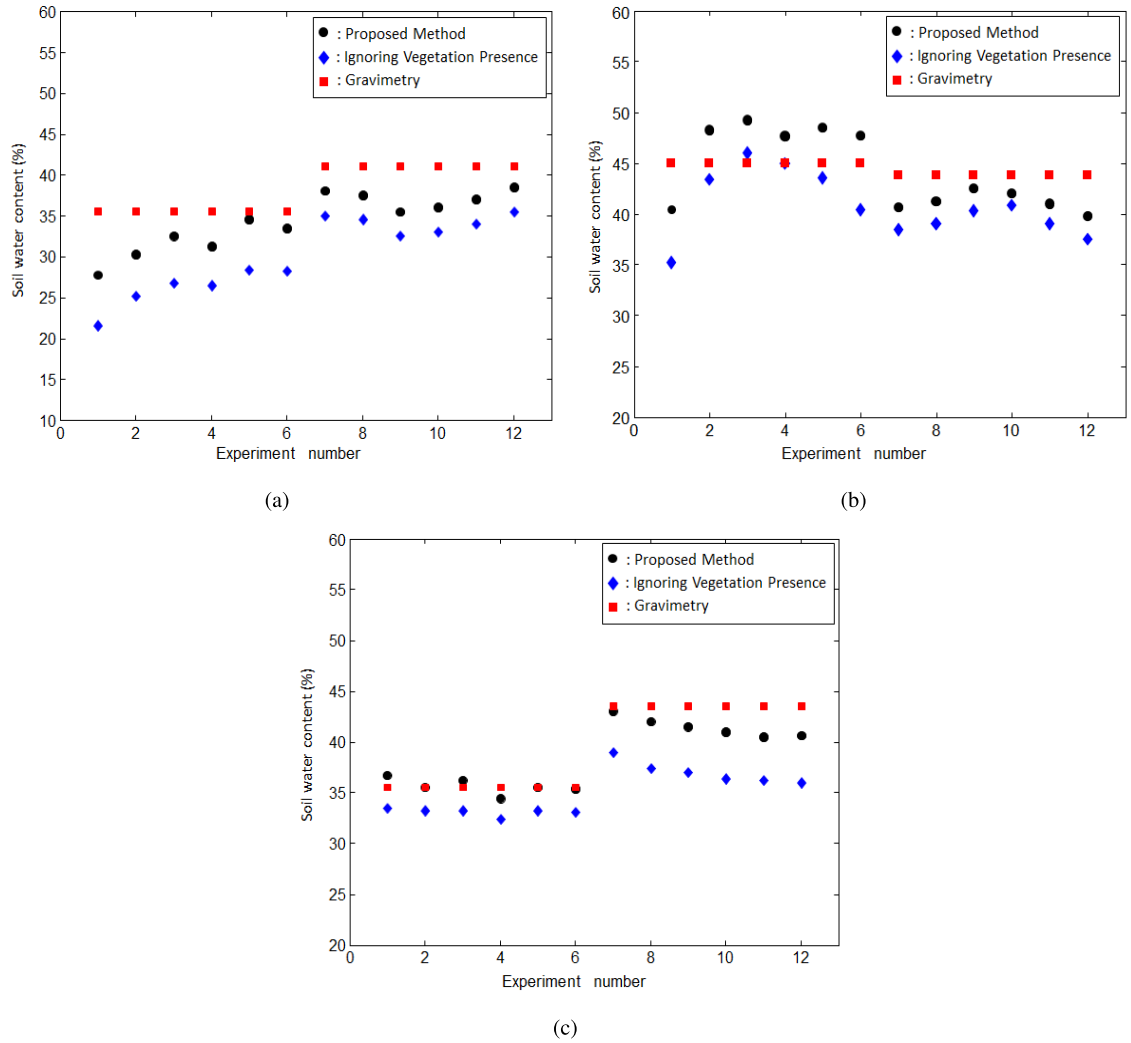

FIGURE 12. Soil water content estimation result. (a). Block I. (b). Block II. (c). Block III.

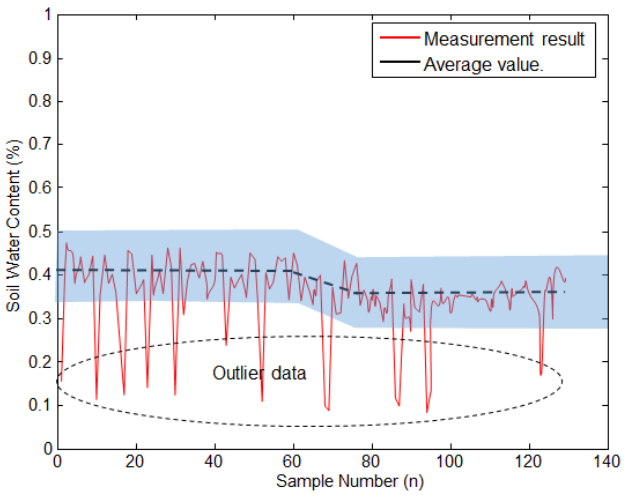

FIGURE 13. Fluctuation in measurement result.

signal, and it complicates the detection process. The method of subtracting the received signal with the receiving signal in the free space direction can eliminate the coupling signal. Therefore, this step is employed to facilitate the identification of the reflected signal.

The proposed inference method, which was developed based on the transmission line model, is used to overcome the effect of plants on the detection results. The proposed inference method is able to increase the detection accuracy up to 96%. The proposed method demonstrates better performance in comparison with the direct conversion method. The transmission line model illustrates that the presence of tea plants influences the estimation results and needs to be addressed. Characterization of plant attenuation is an important step in customizing the proposed method for the case of other crops or plantations.

The experiment results depicted in Fig. 14 show that collecting soil water content data in plantation areas can be carried out quickly using the proposed radar-drone system. The experiment results show that the proposed method is able to collect soil water content data with a speed of 150 m^2/minute.

The drone's ability to maintain a constant flying altitude influences the detection results. The fluctuation of the drone's flying height causes fluctuations in the detection results.

TABLE 3. Radar-drone development.

No.Ref.	Radar-Drone Application	Frequency	Radar Type	Detection Target
[34]	Landmine detection with synthetic aperture radar measurement (side looking method)	1-4 GHz	FMCW	Metal reflector, plastic box, corner reflector.
[35]	Airborne Multi-Channel GPR for Improvised Explosive Devices and Landmine Detection (down looking method)	0.6-3GHz	UWB impulse	landmine
[36]	Low-altitude drone for landmine detection purposes (down looking method)	2 GHz	Impulse	Several kind of landmine
[37]	Retrieve snow-pack properties (down looking method)	0.95-6GHz	UWB Impulse	snowpack
[38]	Through-the-Wall Human Respiration Detection (down looking method)	1.5–6 GHz	UWB Impulse	live victim
[39]	Automotive Radar drone for earth observation (down looking method)	77 GHz	FMCW	corner reflector
[52]	Vital-SAR-imaging with a drone-based hybrid radar system(down looking method)	X band	FMCW and CW	Human respiration and heartbeat
[This Work]	Soil water content estimation in the presence of vegetation	0.5-3GHz	SFCW	Soil water content

Fluctuations in the drone's altitude cause a drop in accuracy of up to 3%. However, the decrease in accuracy can still be tolerated for the needs of precision farming. If, in other plantation or agricultural cases, the environmental conditions cause the drone altitude fluctuations to be more significant, then interesting further studies can be carried out to overcome these problems. The solution can be developed as part of the drone control methods or radar post-processing. Drone flight data records include drone altitude data. The development of compensation methods based on drone altitude data is potential to be applied and can be the next research agenda.

Previous studies on the development of radar drones have been carried out for several applications such as landmine detection, snowpack observation, earth observation, and vital signs. This work also contributes to the development of the application of radar drones, especially in the agriculture field. The Comparison between the proposed radar-drone implementation with previous studies is summarized in Table 3.

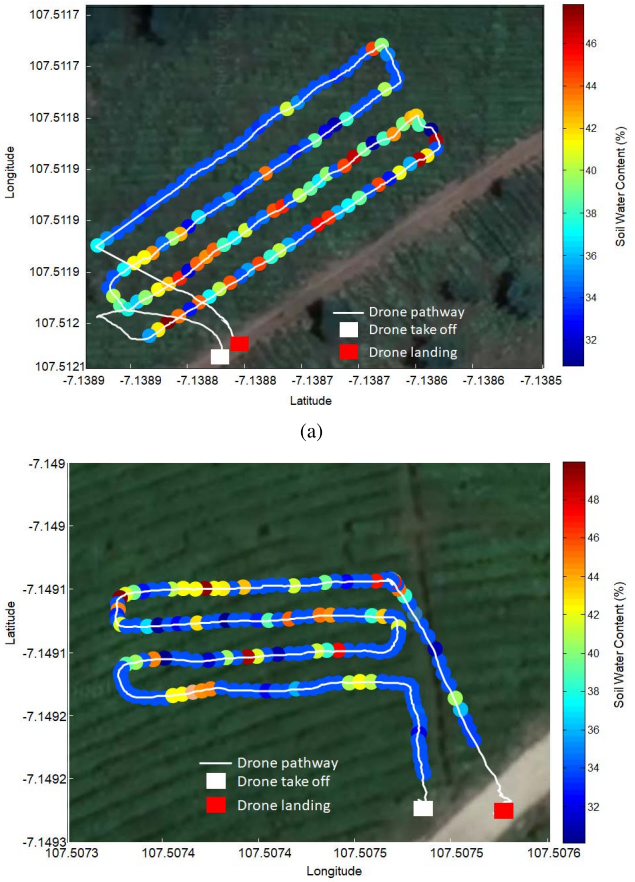

FIGURE 14. Estimated soil water content mapping obtained from radar-drone scanning process. (a). First location. (b) Second location.

IV. CONCLUSION

The UWB radar-drone was proposed for estimating the soil water content of plantation areas with the advantage of being fast and accurate in collecting the soil water content data over a large area. The layer of tea vegetation above the ground significantly affects the radar detection results. The UWB radar system based on SFCW topology was designed with a frequency range of 500 MHz-3 GHz. The radar wave is capable of penetrating the tea vegetation layer. The vegetation gives the effect of attenuation and phase shift to the radar signal that passes through it. The influence of vegetation causes deviations in the measurement results, which are important to overcome. The inference method that considers the presence of the vegetation layer was proposed in this paper.

The proposed inference method was developed based on the wave propagation model on a transmission line. The

transmission line model is elaborated to develop an inference method that is able to accommodate vegetation problems. The transmission line model is used to transform the measured reflection coefficient under the vegetation effect to the ground surface reflection coefficient value. Experiments were carried out by taking case studies on several Blocks in the tea plantations. The tea vegetation over the soil surface that degrades the soil water content detection result has been resolved well by the proposed inference method. The experiment result demonstrates that the proposed method is able to improve the detection results of soil water content. The pro-posed radar drone has an accuracy of 96%.

ACKNOWLEDGMENT

The authors wish to thank the Pusat Penelitian Teh dan Kina, Indonesia, for supporting the experiment in tea plantation located at Ciwidey, West Java, Indonesia.

REFERENCES

[1] R. Lal and K. M. Shukla, *Principles of Soil Physics*. Boca Raton, FL, USA: CRC Press, 2004, pp. 1–11.

[2] T. E. Loynachan, K. W. Brown, T. H. Cooper, and M. H. Milford, *Sustaining Our Soil and Society*. Alexandria, VA, USA: American Geological Institute, 1999, pp. 26–32.

[3] R. Lal and B. A. Stewart, *Soil-Specific Farming: Precision Agriculture, Series: Advances in Soil Science*. Boca Raton, FL, USA: CRC Press, 2021.

[4] J. Neupane and W. Guo, "Agronomic basis and strategies for precision water management: A review," *Agronomy*, vol. 9, no. 87, pp. 1–21, Feb. 2019, doi: 10.3390/agronomy9020087.

[5] H. Vereecken, J. A. Huisman, H. Bogena, J. Vanderborght, J. A. Vrugt, and J. W. Hopmans, "On the value of soil moisture measurements in vadose zone hydrology: A review," *Water Resour. Res.*, vol. 44, no. 4, pp. 253–270, Oct. 2008, doi: 10.1029/2008WR006829.

[6] *Directorate of Food Crops, Horticulture, and Estate Crops Statistics*. Indonesian Tea Statistics, Jakarta, Indonesia, 2020.

[7] J. D. Cooper, *Soil Water Measurement: A Practical Handbook*. Oxford, U.K.: Wiley, 2016, pp. 26–34, doi: 10.1002/9781119106043.

[8] G. Zhou, X. Tao, Y. Sun, R. Zhang, T. Yue, and B. Yang, "A new model for surface soil moisture retrieval from CBERS-02B satellite imagery," *IEEE J. Sel. Topics Appl. Earth Observ. Remote Sens.*, vol. 8, no. 2, pp. 628–637, Feb. 2015, doi: 10.1109/JSTARS.2014.2364635.

[9] B. Li, C. Ti, Y. Zhao, and X. Yan, "Estimating soil moisture with landsat data and its application in extracting the spatial distribution of winter flooded paddies," *Remote Sens.*, vol. 8, no. 1, p. 38, Jan. 2016, doi: 10.3390/rs8010038.

[10] Q. Yuan, H. Xu, T. Li, H. Shen, and L. Zhang, "Estimating surface soil moisture from satellite observations using a generalized regression neural network trained on sparse ground-based measurements in the continental U.S.," *J. Hydrol.*, vol. 580, Jan. 2020, Art. no. 124351, doi: 10.1016/j.jhydrol.2019.124351.

[11] N. Baghdadi, P. Camus, N. Beaugendre, O. M. Issa, M. Zribi, J. F. Desprats, J. L. Rajot, C. Abdallah, and C. Sannier, "Estimating surface soil moisture from TerraSAR-X data over two small catchments in the sahelian part of western Niger," *Remote Sens.*, vol. 3, no. 6, pp. 1266–1283, Jun. 2011, doi: 10.3390/rs3061266.

[12] Y. Gao, M. Gao, L. Wang, and O. Rozenstein, "Soil moisture retrieval over a vegetation-covered area using ALOS-2 L-band synthetic aperture radar data," *Remote Sens.*, vol. 13, no. 19, p. 3894, Sep. 2021, doi: 10.3390/rs13193894.

[13] H. Cui, L. Jiang, S. Paloscia, E. Santi, S. Pettinato, J. Wang, X. Fang, and W. Liao, "The potential of ALOS-2 and sentinel-1 radar data for soil moisture retrieval with high spatial resolution over agroforestry areas, China," *IEEE Trans. Geosci. Remote Sens.*, vol. 60, pp. 1–17, 2022, doi: 10.1109/TGRS.2021.3082805.

[14] C. N. Kovama and K. Schneider, "Vegetation effects on L-band soil moisture retrieval—Lessons learned from 5 years of ALOS PALSAR observations," Presented at the IEEE Int. Geosci. Remote Sens. Symp., Munich, Germany, Jul. 2012, doi: 10.1109/IGARSS.2012.6351321.

[15] F. Jonard, L. Weihermuller, K. Z. Jadoon, M. Schwank, H. Vereecken, and S. Lambot, "Mapping field-scale soil moisture with L-band radiometer and ground-penetrating radar over bare soil," *IEEE Trans. Geosci. Remote Sens.*, vol. 49, no. 8, pp. 2863–2875, Aug. 2011, doi: 10.1109/TGRS.2011.2114890.

[16] J. J. Casanova, S. R. Evett, and R. C. Schwartz, "Design of access-tube TDR sensor for soil water content: Testing," *IEEE Sensors J.*, vol. 12, no. 6, pp. 2064–2070, Jun. 2012, doi: 10.1109/JSEN.2012.2184282.

[17] M. Marilena, M. R. Rivasi, S. Pungnaghi, R. Santangelo, and S. Vincenzi, "Soil volumetric water content measurement using TDR technique," *Annali Di Geofisica*, vol. 39, no. 1, pp. 91–96, Jan. 1996, doi: 10.4401/ag-3953.

[18] Q. Y. Mu, L. T. Zhan, C. P. Lin, and Y. M. Chen, "Non-invasive time domain reflectometry probe for transient measurement of water retention curves in structured soils," *Eng. Geol.*, vol. 264, pp. 31–64, Jan. 2020, doi: 10.1016/j.enggeo.2019.105335.

[19] H. Schafer and N. Beier, "Estimating soil-water characteristic curve from soil-freezing characteristic curve for mine waste tailings using time domain reflectometry," *Can. Geotechnical J.*, vol. 57, no. 1, pp. 73–84, Jan. 2020, doi: 10.1139/cgj-2018-0145.

[20] A. Klotzsche, F. Jonard, and J. Huisman, "Measuring soil water content with ground penetrating radar: A decade of progress," *Vadose Zone J.*, vol. 17, pp. 1–9, Jul. 2018, doi: 10.2136/vzj2018.03.0052.

[21] X. Liu, J. Chen, X. Cui, Q. Liu, X. Cao, and X. Chen, "Measurement of soil water content using ground-penetrating radar: A review of current methods," *Int. J. Digit. Earth*, vol. 12, no. 1, pp. 95–118, Jan. 2019, doi: 10.1080/17538947.2017.1412520.

[22] L. Zhou, D. Yu, Z. Wang, and X. Wang, "Soil water content estimation using high-frequency ground penetrating radar," *Water*, vol. 11, no. 5, p. 1036, May 2019, doi: 10.3390/w11051036.

[23] J. Zheng, X. Teng, J. Liu, and X. Qiao, "Convolutional neural networks for water content classification and prediction with ground penetrating radar," *IEEE Access*, vol. 7, pp. 185385–185392, 2019, doi: 10.1109/ACCESS.2019.2960768.

[24] M. B. Edward, "Remote and ground-based sensor techniquesto map soil properties," *Photogrammetric Eng. Remote Sens. J.*, vol. 69, no. 6, pp. 619–630, Jun. 2003, doi: 10.14358/PERS.69.6.619.

[25] J. A. Huisman, S. S. Hubbard, J. D. Redman, and A. P. Annan, "Measuring soil water content with ground penetrating radar: A review," *Vadose Zone J.*, vol. 2, pp. 476–491, Mar. 2003, doi: 10.2136/vzj2003.4760.

[26] C. Rappaport, "Soil moisture and surface roughness effects in ground penetrating radar detection of land mines," in *IEEE MTT-S Int. Microw. Symp. Dig.*, San Francisco, CA, USA, Jun. 2006, pp. 11–16, doi: 10.1109/MWSYM.2006.249488.

[27] S. M. Ebrahim, N. I. Medhat, K. K. Mansour, and A. Gaber, "Examination of soil effect upon GPR detectability of landmine with different orientations," *NRIAG J. Astron. Geophys.*, vol. 7, no. 1, pp. 90–98, Jun. 2018, doi: 10.1016/j.nrjag.2017.12.004.

[28] A. A. Pramudita and L. Sari, "Extraction model of soil water content information based on least square method for GPR," in *Proc. Int. Symp. Intell. Signal Process. Commun. Syst. (ISPACS)*, Phuket, Thailand, Oct. 2016, pp. 1–5, doi: 10.1109/ISPACS.2016.7824717.

[29] A. Benedetto and F. Benedetto, "Remote sensing of soil moisture content by GPR signal processing in the frequency domain," *IEEE Sensors J.*, vol. 11, no. 10, pp. 2432–2441, Oct. 2011, doi: 10.1109/JSEN.2011.2119478.

[30] F. Cui, J. Ni, Y. Du, Y. Zhao, and Y. Zhou, "Soil water content estimation using ground penetrating radar data via group intelligence optimization algorithms: An application in the northern Shaanxi coal mining area," *Energy Explor. Exploitation*, vol. 39, no. 1, pp. 318–335, Jan. 2021, doi: 10.1177/0144598720973369.

[31] G. Serbin and D. Or, "Ground-penetrating radar measurement of soil water content dynamics using a suspended horn antenna," *IEEE Trans. Geosci. Remote Sens.*, vol. 42, no. 8, pp. 1695–1705, Aug. 2004, doi: 10.1109/TGRS.2004.831693.

[32] D. J. Daniel, *Ground Penetrating Radar*, 2nd ed. London, U.K.: IEE Press, 2004.

[33] S. Lambot, E. C. Slob, I. van den Bosch, B. Stockbroeckx, B. Scheers, and M. Vanclooster, "Vanclooster, estimating soil electric properties from monostatic ground-penetrating radar signal inversion in the frequency domain," *Water Resour. Res.*, vol. 40, pp. 1–12, Apr. 2004, doi: 10.1029/2003WR002095.

[34] M. Schartel, R. Burr, W. Mayer, N. Docci, and C. Waldschmidt, "UAV-based ground penetrating synthetic aperture radar," in *IEEE MTT-S Int. Microw. Symp. Dig.*, Apr. 2018, pp. 1–4, doi: 10.1109/ICMIM.2018.8443503.
[35] M. García-Fernández, Y. López, and F. L.-H. Andrés, "Airborne multi-channel ground penetrating radar for improvised explosive devices and landmine detection," *IEEE Access*, vol. 8, pp. 165927–165943, 2020, doi: 10.1109/ACCESS.2020.3022624.
[36] J. Colorado, C. Devia, M. Perez, I. Mondragon, D. Mendez, and C. Parra, "Low-altitude autonomous drone navigation for landmine detection purposes," in *Proc. Int. Conf. Unmanned Aircr. Syst. (ICUAS)*, Jun. 2017, pp. 540–546, doi: 10.1109/ICUAS.2017.7991303.
[37] A. Vergnano, D. Franco, and A. Godio, "Drone-borne ground-penetrating radar for snow cover mapping," *Remote Sens.*, vol. 14, no. 7, p. 1763, Apr. 2022, doi: 10.3390/rs14071763.
[38] B. P. A. Rohman, M. Andra, and M. Nishimoto, "Through-the-wall human respiration detection using UWB impulse radar on hovering drone," *IEEE J. Sel. Topics Appl. Earth Observ. Remote Sens.*, vol. 14, pp. 6572–6584, 2021, doi: 10.1109/JSTARS.2021.3087668.
[39] C. Weber, J. von Eichel-Streiber, J. Rodrigo-Comino, J. Altenburg, and T. Udelhoven, "Automotive radar in a UAV to assess Earth surface processes and land responses," *Sensors*, vol. 20, no. 16, p. 4463, Aug. 2020, doi: 10.3390/s20164463.
[40] F. N. Aliefudin, D. Arseno, and A. Pramudita, "Wall effect compensation for detection improvement of through the wall radar," Presented at the Int. Conf. Inf. Commun. Technol. (ICOIACT), Yogyakarta, Indonesia, Jul. 2019, doi: 10.1109/ICOIACT46704.2019.8938470.
[41] Y. Zhou, C. Huang, H. Liu, D. Li, and T.-K. Truong, "Front-wall clutter removal in through-the-wall radar based on weighted nuclear norm minimization," *IEEE Geosci. Remote Sens. Lett.*, vol. 19, pp. 1–5, 2022, doi: 10.1109/LGRS.2020.3034568.
[42] G. C. Topp, J. L. Davis, and A. P. Annan, "Electromagnetic determination of soil water content: Measurements in coaxial transmission lines," *Water Resour. Res.*, vol. 16, no. 3, pp. 574–582, Jun. 1980, doi: 10.1029/WR016i003p00574.
[43] S. Hensley, "L-band and P-band studies of vegetation at JPL," Presented at the IEEE Radar Conf., Johannesburg, South Africa, Oct. 2015, doi: 10.1109/RadarConf.2015.7411937.
[44] P. S. Narvekar, D. Entekhabi, S.-B. Kim, and E. G. Njoku, "Soil moisture retrieval using L-band radar observations," *IEEE Trans. Geosci. Remote Sens.*, vol. 53, no. 6, pp. 3492–3506, Jun. 2015, doi: 10.1109/TGRS.2014.2377714.
[45] S. B. Kim, H. Huang, T. H. Liao, and A. Colliander, "Estimating vegetation water content and soil surface roughness using physical models of L-band radar scattering for soil moisture retrieval," *Remote Sensing*, vol. 10, no. 4, p. 556, 2018, doi: 10.3390/rs10040556.
[46] A. A. Pramudita, T. O. Praktika, and S. Jannah, "Radar modeling experiment using vector network analyzer," Presented at the Int. Symp. Antennas Propag. (ISAP), Osaka, Japan, Jan. 2021, doi: 10.23919/ISAP47053.2021.9391495.
[47] I. Magdy, *Electromagnetic Field and Wave*. Hoboken, NJ, USA: Prentice-Hall, 1992.
[48] H. Oraizi and M. Afsahi, "Analysis of planar dielectric multilayers as FSS by transmission line transfer matrix method (TLTMM)," *Prog. Electromagn. Res.*, vol. 74, pp. 217–240, 2007, doi: 10.2528/PIER07042401.
[49] H. Oraizi and M. Afsahi, "Transmission line modeling and numerical simulasion for the analysis and optimum design of metamaterial multilayer structures," *Prog. Electromagn. Res. B*, vol. 14, pp. 263–283, 2009, doi: 10.2528/PIERB09022506.
[50] M. Ni, Q. Sheng, and X. Zhang, "Design and calibration of soil water content sensor based on dual frequency excitation," *IEEE Sensors J.*, vol. 21, no. 24, pp. 27540–27548, Dec. 2021, doi: 10.1109/JSEN.2021.3124785.
[51] J. Mizuguchi, J. C. Piai, J. A. de França, M. B. de Morais França, K. Yamashita, and L. C. Mathias, "Fringing field capacitive sensor for measuring soil water content: Design, manufacture, and testing," *IEEE Trans. Instrum. Meas.*, vol. 64, no. 1, pp. 212–220, Jan. 2015, doi: 10.1109/TIM.2014.2335911.
[52] J. Yan, Z. Peng, H. Hong, H. Chu, X. Zhu, and C. Li, "Vital-SAR-imaging with a drone-based hybrid radar system," *IEEE Trans. Microw. Theory Techn.*, vol. 66, no. 12, pp. 5852–5862, Dec. 2018, doi: 10.1109/TMTT.2018.2874268.

ALOYSIUS A. PRAMUDITA (Member, IEEE) was born in Klaten, Indonesia, in 1977. He received the B.S. degree in electrical engineering from Gadjah Mada University, Indonesia, in 2000, and the M.S. and Ph.D. degrees in electrical engineering from the Bandung Institute of Technology, Indonesia, in 2005 and 2009, respectively. From 2002 to 2016, he was a Lecturer and a Researcher with Atma Jaya Catholic University, Indonesia, where he was the Head of the Electrical Engineering Department, from 2013 to 2016, and the Head of the Electrical Engineering Graduate Program, from 2016 to 2017. Since 2017, he has been with the Telecommunication Engineering Department, Telkom University, Bandung, Indonesia. Since 2020, he has been the Director of the Internet of Things Research Center, Telkom University, that focuses on intelligent sensing research area. He is currently a member of the Telkom University Radar Research Group. He is also the Head of the Satellite Communication and Radar Laboratory, Telkom University. His research interests include antenna theory and design for telecommunication and radar, electromagnetics and wave application, and radar system for contactless sensor. He serves as a reviewer for several technical journals and conferences in his interest area.

YUYU WAHYU was born in Bandung, Indonesia, in February 1962. He received the Insinyur (Ir.) degree from the School of Electrical and Informatics Engineering, Institut Teknologi Bandung, Bandung, in 1990, the M.Eng. (M.T.) degree in telecommunication information system from the Electrical Engineering Study Program, School of Electrical and Informatics Engineering, Institut Teknologi Bandung, in 2000, and the Ph.D. degree in global information and telecommunication studies from the School of Electrical and Informatics Engineering, Institut Teknologi Bandung, in 2010. He has been with the Telecommunications Research Center, Strategic Electronics, Components and Materials (Telkoma), Indonesian Institute of Sciences—LIPI (now the Research Center for Electronics and Telecommunications, LIPI), since 1991. He was the Head of the Telecommunications and Radio Laboratory, from 2000 to 2003, and research facilities, from 2010 to 2016. He has been the Chair of the Research Group of Antennas and Propagation, since 2014. Since 2019, he has been appointed as a Research Professor in telecommunications transmission. He followed a number of activities related to his field of competence, including Guest Research, Okayama, Japan, in 2003; and for one and half months on the topic of active antenna and radar training, in 2006 and 2007, at IRCTR-TU, Delft, The Netherlands. He has been conducting FMCW radar research, since 2006, and electronic support measure (ESM), from 2015 to 2018. He has been participating in professional organizations, including Himpenindo (Association of Indonesian Researchers), since 2018; the Indonesian Radar Association, since 2008; and the IEEE Antenna and Propagation Society, since 2010.

SYAMSUL RIZAL received the bachelor's degree in telecommunication engineering from Telkom University, Bandung, in 2011, and the master's and Ph.D. degrees from the IT Convergence Department, Kumoh National Institute of Technology, South Korea. He was doing his postdoctoral research at DGIST, South Korea, and doing his research on unmanned vehicle using machine learning. He is currently working as a Lecturer in telecommunication engineering with Telkom University. His research interests include machine learning and embedded systems.

MURMAN D. PRASETIO was born in Surabaya, Indonesia, in 1986. He graduated in electrical engineering from the Sepuluh Nopember Institute of Technology, Surabaya, in 2009. He received the master's degree in industrial management from the National Taiwan University of Science and Technology (NTUST), in June 2012, and the Ph.D. degree in system cybernetics and engineering from Hiroshima University, in 2019. He was a Lecturer and a Researcher with the Institute Technology Kalimantan, from 2015 to 2016, and then continues his journey. He has been with Telkom University, Bandung, Indonesia, since 2019. He was a member of the Automation Laboratory, under group of production and manufacturing system. Since April 2020, he has been the Leader of production and manufacturing system. His main research interests include machine learning, devices automation, and industrial development technology.

AGUNG N. JATI received the graduate degree in electrical engineering and the master's degree in telecommunication engineering from Institut Teknologi Telkom (currently known as Telkom University), Bandung, Indonesia, in 2009 and 2012, respectively. He is currently pursuing the Ph.D. degree with the School of Electrical Engineering and Informatics, Institut Teknologi Bandung, Bandung. He was a Supervisor of the Intelligent Robotic Research Group, Telkom University, from 2012 to 2018. He is a Lecturer with the School of Electrical Engineering, Telkom University. He is also a member of the Internet of Things Research Center, Telkom University. His research interests include theoretical and application of sensor network, mobile robotic, and embedded systems.

RESTU WULANSARI was born in Jakarta, in December 1986. She received the bachelor's degree from the Department of Soil Science, Gadjah Mada University, in 2019, and the master's degree in soil science and soil fertility from Padjadjaran University, in 2021. She is currently a Soil and Plant Nutrition Researcher, specializing in soil science, agroclimatology, and hydrology at the Tea and Quinine Research Center, Indonesia. She attended the short course "Program in Tea Plantation Management" at the Kothari Agricultural Management Center (KAMC), Tamil Nadu, India, in 2015. She has participated in the Green Tea Development Training, Japan, in 2019. Her research interests include fertility and soil conservation and the development of IT-based technology for tea and quinine. She is active in writing articles in various national and international scientific journals and serves as a reviewer for several journals and committees in several training and conferences.

HARFAN H. RYANU (Member, IEEE) received the B.S. degree in telecommunication engineering from the Telkom Institute of Technology, Bandung, Indonesia, in 2011, and the M.E. degree in telecommunication engineering from The University of Sydney, Sydney, NSW, in 2018. He is currently a Lecturer with the School of Electrical Engineering, Telkom University. He is also with the Basic Transmission Laboratory. His research interests include RF device, especially in remote sensing area, radar, and antenna, and has been published some papers and journals in those fields on national journal.